

# Chapter 3

## Characterization of

## *Paracoccus* sp. W1b biofilm

### 3.1. Introduction

A conceptual framework for biofilm formation as a microbial development was provided by O'Toole et al. (2000). However, Klausen et al. (2006) proposed that ecological adaptation of individual cells drive the evolution of biofilm spatial structure. Certain nutritional factors are known to influence biofilm development (Geesey et al. 2000; Prakash et al. 2003; Sauer et al. 2004; Song and Leff, 2006; Schlag et al. 2007; Monds et al. 2007; Yang et al. 2007). Impact of nutrient composition on architecture and physiochemistry of degradative biofilm community has also been reported by Moller et al. (1997). In order to exploit full potential of biofilms in wastewater treatment, it is necessary to understand the influence of various environmental factors on biofilm structure, and in turn their activity.

In the present objective, *Paracoccus* sp.W1b, isolated from the denitrifying reactor sludge (DaS) was used. The isolate was found to be an efficient denitrifier as compared to the other isolated cultures mentioned in the previous chapter. *Paracoccus* species are reported to form biofilm (Neef et al. 1996; Kim et al. 2004) and some *Paracoccus* species are also known to have attributes of degrading xenobiotics (Urakami et al. 1990; Siller et al. 1996; Vasilyeva et al. 2003; Peng et al. 2008; Xu et al. 2008). The genus *Paracoccus* are metabolically versatile Gram negative coccoid bacteria having the apparatus to denitrify nitrogenous oxides under anoxic conditions (Baker et al. 1998).

Plackett-Burman statistical design of experiment approach was adopted to investigate the effect of seven different nutrient components on the *Paracoccus* sp. W1b biofilm in this study. Screening of nutrients by one-factor-at-a-time is time consuming, while a statistical approach helps to study the effect of several nutrient factors simultaneously. Plackett-Burman is a two level fractional factorial design in which each factor is tested an equal number of times at its high and low values and influence of various factors can be determined in small number of trials (Plackett & Burman 1946). As such, use of statistical designs for optimizing nutritional conditions to maximize yield is an established practice in industrial fermentation (Srinivas et al. 1994; Gohel et al. 2006; Akolkar et al. 2008).

The objective of this study was to investigate the influence of nutritional components on the biofilm of *Paracoccus* sp. W1b. It was hypothesized that the nutrients also influence the architecture of the biofilm which in turn affect the activity.

## 3.2. Materials and Methods

### 3.2.1. Bacterial strain and culture conditions

A denitrifying isolate, W1b, identified in our laboratory as *Paracoccus* sp. W1b was used in this study. Culture was maintained and inoculum prepared in peptone nitrate medium (PNB). 24 hour old culture was centrifuged, washed and resuspended in phosphate buffered saline (PBS) before inoculation. Biofilm experiments were performed in MM2 medium consisting of Sodium succinate 7.9g, MgSO<sub>4</sub>·7H<sub>2</sub>O 0.2g, K<sub>2</sub>HPO<sub>4</sub> 0.2g, FeSO<sub>4</sub>·7H<sub>2</sub>O 0.05g, CaCl<sub>2</sub>·2H<sub>2</sub>O 0.02g, MnCl<sub>2</sub>·4H<sub>2</sub>O 0.002g, NaMoO<sub>4</sub>·2H<sub>2</sub>O 0.001g, KNO<sub>3</sub> 1.0g, Yeast extract 1.0g, pH 7.0, Distilled Water 1000 ml. All experiments were performed at 30°C in static/anoxic condition.

### 3.2.2. Plackett-Burman statistical design to screen nutrient components influencing biofilm

The Plackett-Burman design was according to Montgomery (1997). A total of seven media components were selected for the study with each component/variable being represented at two levels, high (+) and low (-) in twelve different media as shown in Tables 3.1 & 3.2. Nutrient concentrations were selected based on single parametric studies on biofilm formation of *Paracoccus* sp. W1b in our lab. Each column represents a medium and each row represents an independent/assigned or dummy/unassigned variable with equal number of positive and negative signs. The effect of each variable was determined by following equation:

$$E(X_i) = \frac{2(\sum Mi^+ - \sum Mi^-)}{N} \quad (1)$$

Where,  $E(X_i)$  is the concentration effect of the tested variable.  $Mi^+$  and  $Mi^-$  are the biofilm intensity or structural parameters in the medium where the variable ( $X_i$ ) measured were

present at high and low concentrations respectively, and  $N$  is the number of media. Experimental error was estimated by calculating the variance among the unassigned variables as follows:

$$V_{\text{eff}} = \frac{\sum(Ed)^2}{n} \quad (2)$$

Where,  $V_{\text{eff}}$  is the variance of the concentration effect,  $Ed$ , the concentration effect for the unassigned variable and  $n$  is the number of unassigned variables. The standard error (S.E.) of the concentration effect is the square root of the variance of an effect.

$$\text{S.E} = \text{Square root of } V_{\text{eff}} \quad (3)$$

The significance level ( $p$  value) of each concentration effect was determined by student's  $t$  test:

$$t(X_i) = \frac{E(X_i)}{\text{S.E}} \quad (4)$$

Where,  $E(X_i)$  is the effect of variable  $X_i$ .

**Table 3.1.** Plackett-Burman design matrix

Variables/Medium	A	B	C	D	E	F	G	H	I	J	K	L
X1	1	-1	1	-1	-1	-1	1	1	1	-1	-1	1
X2	1	1	-1	1	-1	-1	-1	1	1	1	-1	-1
X3	-1	1	1	-1	1	-1	-1	-1	1	1	1	-1
X4	1	-1	1	1	-1	1	-1	-1	-1	1	1	-1
X5	1	1	-1	1	1	-1	1	-1	-1	-1	1	-1
X6	1	1	1	-1	1	1	-1	1	-1	-1	-1	-1
X7	-1	1	1	1	-1	1	1	-1	1	-1	-1	-1
D1	-1	-1	1	1	1	-1	1	1	-1	1	-1	-1
D2	-1	-1	-1	1	1	1	-1	1	1	-1	1	-1
D3	1	-1	-1	-1	1	1	1	-1	1	1	-1	-1
D4	-1	1	-1	-1	-1	1	1	1	-1	1	1	-1

X=Assigned variables D=Unassigned variables

**Table 3.2.** Variables with media components and their concentrations

Variables	Components	+ values (mM)	- values (mM)
X1	KNO <sub>3</sub>	100.0	0.1
X2	Succinate	50.0	0.5
X3	MgSO <sub>4</sub>	15.0	0.15
X4	FeSO <sub>4</sub>	1.0	0.1
X5	K <sub>2</sub> HPO <sub>4</sub>	10.0	0.01
X6	CaCl <sub>2</sub>	15.0	0.15
X7	MnCl <sub>2</sub>	1.0	0.01

### 3.2.3. Microtiter plate assay for biofilm quantification

Biofilm formation was assayed by measuring the bacterial biomass adhered to microtiter wells. 1ml of MM2 medium was inoculated with  $10^8$  cells in 24 wells polystyrene microtiter plate. After the incubation period, the wells were rinsed five times with 1.5ml of sterile PBS to remove any adhering planktonic cells. The biofilm was then stained with 1.5ml of 1% crystal violet for 45 min, rinsed five times with 1.5ml of water and destained with 70% ethanol for 15min. Absorbance of the solution was measured at 595nm.

### 3.2.4. Confocal microscopy and image analysis

Polystyrene slides with 2 x 2 cm diameter were used for biofilm formation, which were incubated in petri dish containing medium at 30°C for 24 hours in static condition. The slides were then rinsed with sterile PBS (pH 7.4) and stained with LIVE/DEAD baclight® according to manufacturer's instructions. Image acquisition was done at 40X in Zeiss (LSM 510 Meta) confocal laser scanning microscope (CSLM). Two to four independent slides and three to seven fields from each slide were randomly chosen to acquire images with constant microscopic settings; overall 245 images were processed. Raw images were processed by IMARIS and Adobe Photoshop softwares. Quantification of biofilm parameters were done

by COMSTAT program written as a script in MATLAB 5.1 (Heydorn et al. 2000). Live to dead ratio was calculated by measuring densities of red and green fluorescence images by ImageJ, a NIH freeware (<http://rsb.info.nih.gov/ij/index.html>).

### 3.2.5. Environmental scanning electron microscopy (ESEM)

Biofilm formed polystyrene slides were treated according to Priester et al. (2007) with few modifications. Slides were stained by 0.05% ruthenium red and 2.5% glutaraldehyde (used as a fixative) in 0.1M HEPES buffer (pH 7.3, Sigma chemical) for 30 minutes. Further, the slides were washed with HEPES buffer, dried and taken for observation under the ESEM (XL-30, Philips, Netherlands).

### 3.2.6. Biofilm experiments with chelator treatment

Effect of ethylenediaminetetraacetic acid (EDTA) on biofilm formation was assessed by adding 0.0 to 10.0 mM concentration of EDTA in MM2 medium and biofilm formation assayed by the microtiter plate technique.

To investigate influence of chelators on biofilm of various ages, the following procedure was followed. Biofilm was grown in petri dishes containing polystyrene slides in MM2, MM2-Ca (MM2 medium containing 10mM CaCl<sub>2</sub>) or MM2-Mg (MM2 medium containing 10mM MgSO<sub>4</sub>) media. Biofilm slides of 6, 12, 18 and 30 hours were rinsed with PBS and treated with 10mM EDTA (for MM2 or MM2-Mg grown biofilms) or EGTA (for MM2-Ca grown biofilm) for 30 minutes. Control biofilms were treated with PBS. The biofilm was then stained with LIVE/DEAD baclight<sup>®</sup> (Invitrogen) for confocal microscopy and biomass was measured by COMSTAT. The percentage of biomass reduced by chelator treatment was calculated by:

$$\frac{(B1 - B2) 100}{B1} \quad (5)$$

Where, B1 = Average biomass in PBS treated biofilm, B2 = Average biomass in chelator treated biofilm

### 3.2.7. Bacterial Adherence to Hydrocarbons (BATH) Assay

The BATH test was carried out to analyse the cell surface hydrophobicity. *Paracoccus* sp. W1b was inoculated in MM2 and MM2-Mg medium and incubated at 30°C for 30 hours. Cells were pelleted down and washed once with PBS. Pellet was dissolved in PBS such that the Absorbance at 600 nm is between 0.4- 0.6. 6 ml of this solution was taken in a clean test tube. To this 300 µl of hexane was added, vortexed vigorously for 10 seconds and allowed to stand for 30 min. Absorbance at 600 nm of the aqueous phase was measured. The assay was done in nine replicates and the standard error of the mean was calculated. Cell hydrophobicity is referred to the percentage of cells that migrates towards the organic phase.

### 3.2.8. Fatty acid Methyl Esters (FAME)

Collection of biofilm subpopulation cells in MM2-Mg was done as follows. Biofilm was allowed to grow in MM2-Mg medium for 30 hours at 30°C on large sterile polystyrene cells. The biofilm slides were treated with EDTA for 15 minutes and the eluted cells were immediately centrifuged for 5 minutes, washed twice with PBS and dissolved in 0.5 ml sterile distilled water. The Cell that still adhered to the substratum were also scraped off with a rubber policeman and washed twice with PBS and dissolved in 0.5 ml sterile distilled water.

Extraction of the FAME was done by adding 1 ml of 15% NaOH in 50% methanol to the cell suspension and incubating it in 100°C water bath for 30 minute. This was further cooled to ambient temperature. To this saponified mixture, 3.75 ml of Chloroform-Methanol (1:2 v/v) (Bligh/Dyer mixture) was added and mixed well in a separating funnel. After the separation, the lower phase was collected to which 2.5 ml of BF<sub>3</sub> -Methanol mixture was added and boiled for 2 min. 4 ml of n- heptane was added to this mixture and boiled for 8 min. The mixture was cooled, and saturated NaCl solution was added up to the neck of the flask. The uppermost clear heptane layer was collected containing FAME and transferred into sample vials. The sample was injected into the GC-MS and the peaks were identified by comparing with the inbuilt library of the instrument.

### 3.3. Results

The isolate *Paracoccus* sp. W1b was observed to be an efficient denitrifier which could also reduce and tolerate nitrate at high concentrations. Furthermore the biofilm formation characteristics of this isolate were analyzed in this chapter.

#### 3.3.1. Biofilm formation by *Paracoccus* sp. W1b

The *Paracoccus* sp. W1b isolate was grown in a petri dish containing MM2 medium and a polystyrene slide for the formation of biofilm on its surface. The biofilm formation was checked by staining the slide with crystal violet and observed under a brightfield microscope (Olympus CX41).

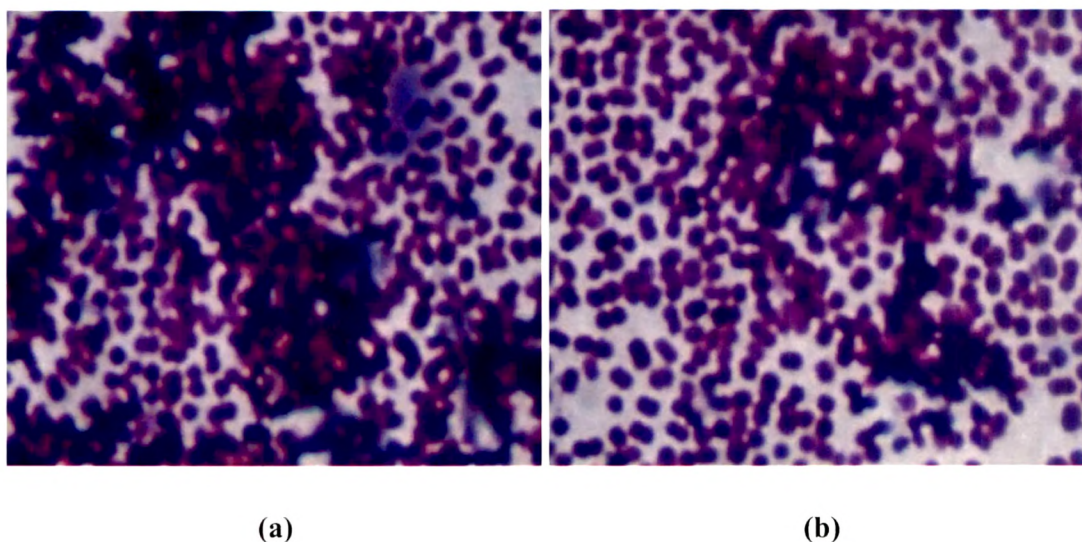


**Fig. 3.1.** Representative images of the biofilm formation by *Paracoccus* sp. W1b on a polystyrene slide observed under a brightfield (Olympus CX41) microscope at 100X magnification

Clusters of cell adhered to the slide was observed, suggesting formation of a biofilm by the *Paracoccus* sp. W1b isolate (Fig. 3.1). The biofilm was further observed through the environmental scanning electron microscope (ESEM), where, at high magnification of 10000 and 15000 X, the cell clusters of *Paracoccus* sp. W1b were viewed and the dimension of each cell was observed to be of nearly 1  $\mu\text{m}$  in diameter (Fig. 3.2).

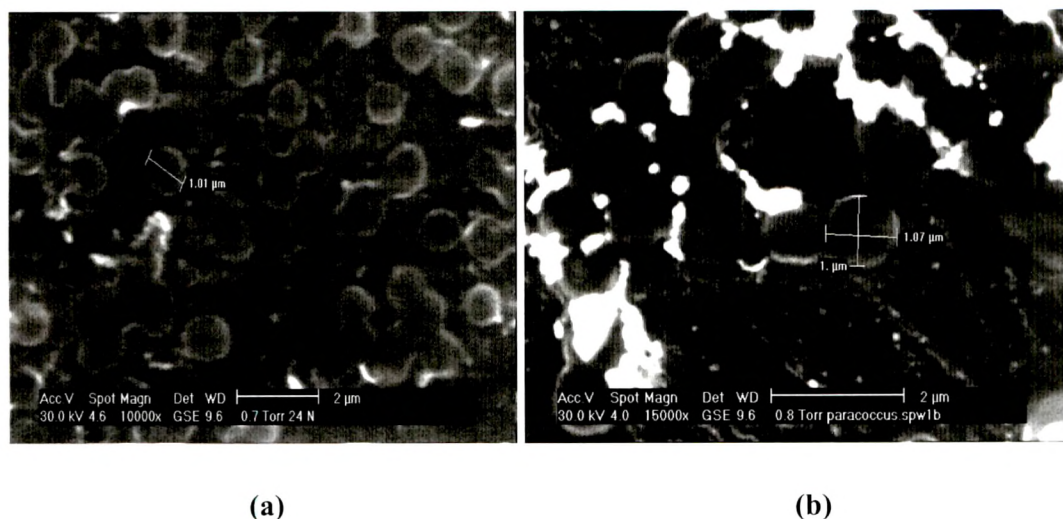


**Fig. 3.2.** Representative Environmental Scanning Electron Microscopic (ESEM) images showing the biofilm formed by *Paracoccus* sp. W1b on polystyrene slides. (a) 10000X and (b) 15000X magnification

### 3.3.2. Nutrients influence Biofilm formation

Furthermore, influence of different nutrient concentrations on the formation of biofilm was assessed in the 24 wells microtitre plate assay. The biomass in terms of intensity of the eluted crystal violet from microtiter plates were considered as the measure of biofilm formation. It was observed that the divalent cations, magnesium, calcium and manganese increased the biofilm formation at their higher concentration whereas iron decreased the formation of biofilm at higher concentration (Fig. 3.3). Succinate too increased the biofilm formation with increasing concentrations (Fig. 3.3). However, the amount of biofilm formed was greater with higher concentration of magnesium. Further, the influence of nutrients on the formation of biofilm was analyzed by the Plackett-Burman statistical experiment.

Results of Plackett-Burman experiment for effect of nutrients on biofilm formation, as shown in Fig. 3.4a indicate that medium B produced high biofilm, followed by media F and H. The effect of different components on the biofilm formation and planktonic growth could further be interpreted by calculating the  $E(X_i)$  values. Fig. 3.4b represents  $E(X_i)$  values calculated for the biofilm formation. Positive  $E(X_i)$  value of the variable is considered to

induce biofilm formation at higher concentration tested, and when negative, the variable is considered to induce biofilm formation at lower concentration. Succinate,  $MgSO_4$ ,  $CaCl_2$ , and  $MnCl_2$  showed positive  $E(X_i)$  value ( $p \leq 0.1$ ), thus significantly inducing the biofilm formation at higher concentrations.

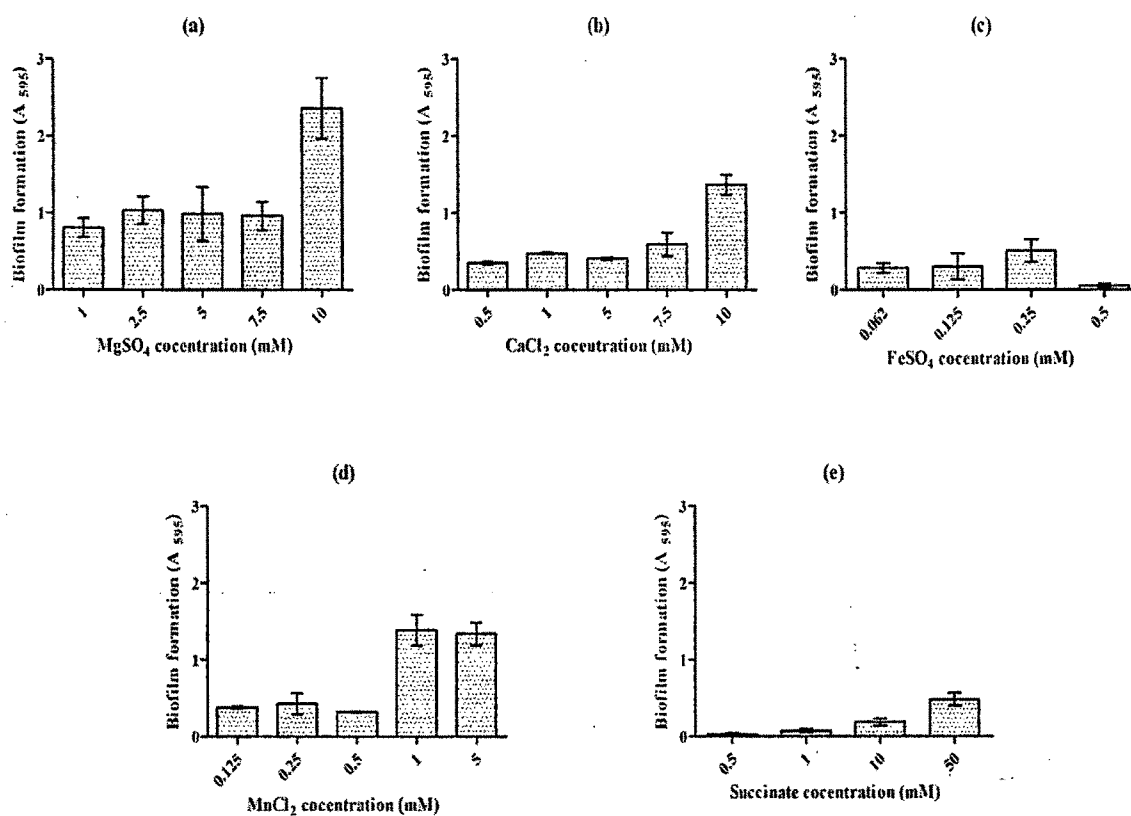


**Fig. 3.3.** Influence of different nutrient concentrations on the biofilm formation by *Paracoccus* sp. W1b

$FeSO_4$  showed a negative  $E(X_i)$  value ( $p \leq 0.05$ ) inducing biofilm formation at lower concentrations. Only succinate showed nearly significant ( $p = 0.112$ ) positive influence on the planktonic growth.

### 3.3.3. Nutrients modulate biofilm architecture

Effect of nutrients on biofilm architecture was analyzed by studying their influence on six different biofilm structural parameters deduced from CSLM images (Fig. 3.5 a-l). Results of

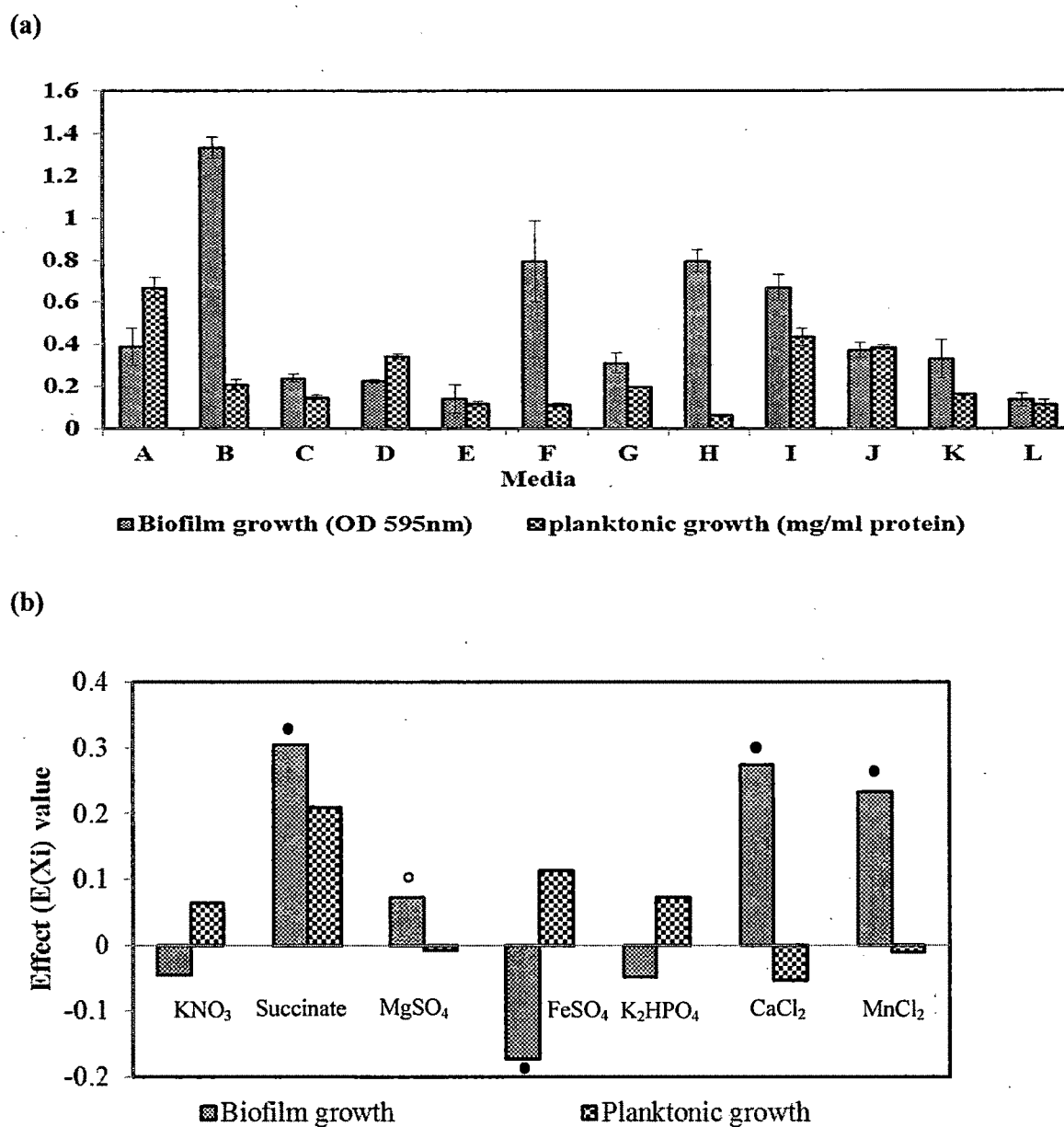


**Fig. 3.4.** Nutrient components influencing *Paracoccus* sp. W1b biofilm formation (a) Biofilm formation and planktonic growth in different media of Plackett-Burman experiment. Bars represent average values of three independent experiments. Error bars represent standard deviations (b) Effect (E(Xi)) values of the nutrient components on biofilm formation and Planktonic growth.

● Significant at  $p < 0.05$ . ○ Significant at  $p < 0.1$

biofilm quantification for twelve different media of Plackett-Burman design are given in Table 3.3. Medium C produced high biomass, average thickness, substratum coverage and low roughness coefficient, implying formation of a thick and homogenous biofilm. Media A and F showed decreased biomass, average thickness, maximum thickness and substratum coverage; high values of roughness coefficient and surface to biovolume ratio, entailing the formation of an uneven flat biofilm.

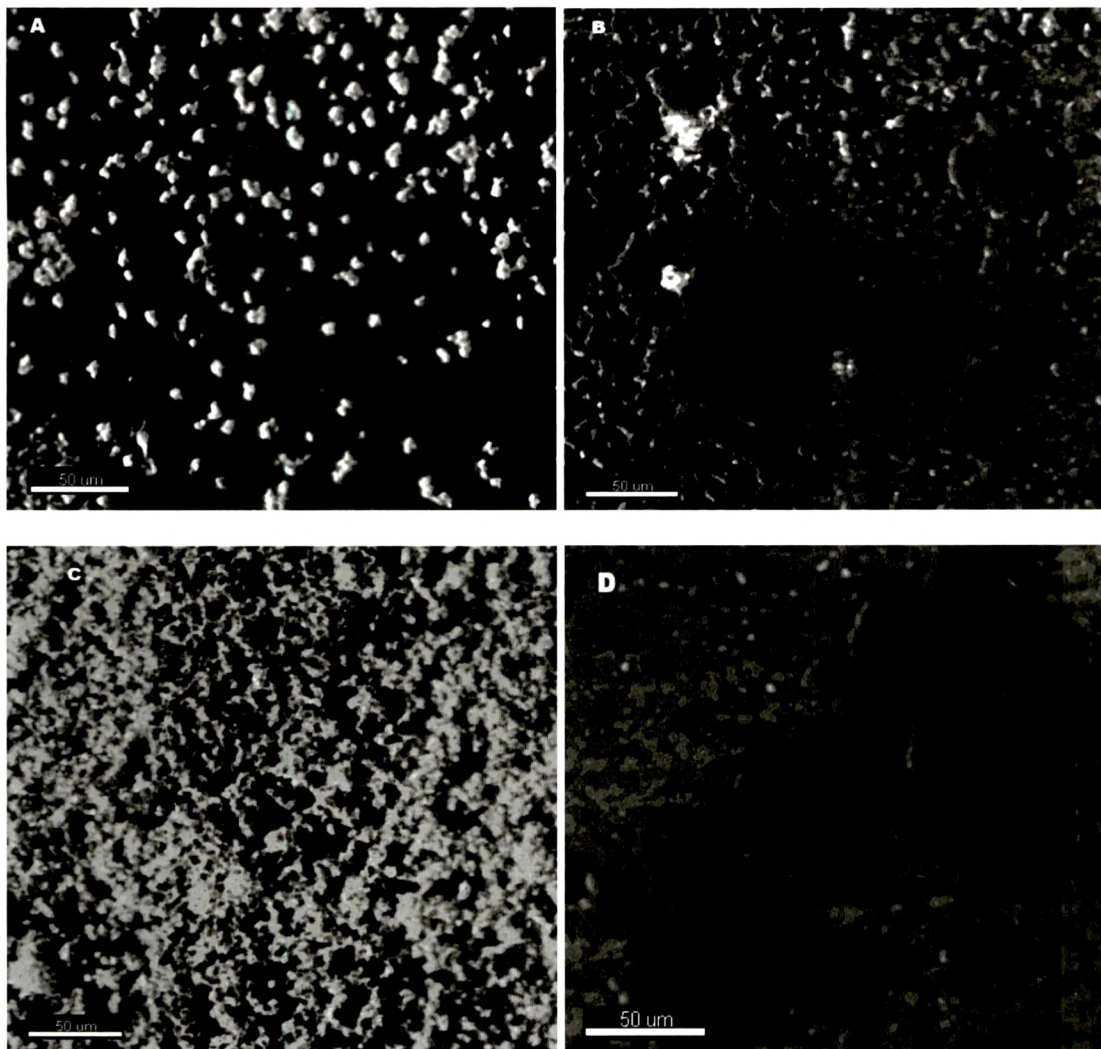
Table 3.4 shows effect ( $E(X_i)$ ) and corresponding p-values of seven different nutrient components on the six biofilm parameters. The positive  $E(X_i)$  value means that the particular medium component induces corresponding biofilm parameter at its higher concentration and negative value implies lower concentration of medium component has a positive effect on the biofilm parameter. If surface to biovolume ratio is affected positively, it means that high fraction of cells in biofilm are exposed to the bulk liquid and negative effect implies that the fraction of cells exposed to bulk liquid is low.

Succinate affected biomass negatively ( $p < 0.05$ ) whereas the maximum thickness ( $p < 0.05$ ), roughness coefficient ( $p < 0.1$ ) and surface to biovolume ratio ( $p < 0.1$ ) positively. This indicates that the biofilm formed at high succinate concentrations are uneven in thickness with more cells exposed to the bulk liquid. Magnesium affected the biomass ( $p < 0.05$ ), maximum thickness ( $p < 0.05$ ) positively and surface to biovolume ratio negatively ( $p < 0.05$ ), suggesting that the cells are densely clustered. Nitrate affected the biomass positively ( $p = 0.109$ ). Calcium influenced surface to biovolume ratio, biomass and maximum thickness positively, ( $p = 0.06$ ,  $p = 0.178$  and  $0.162$  respectively) implying that a thick biofilm was formed at high calcium levels with more cells exposed to the bulk liquid.

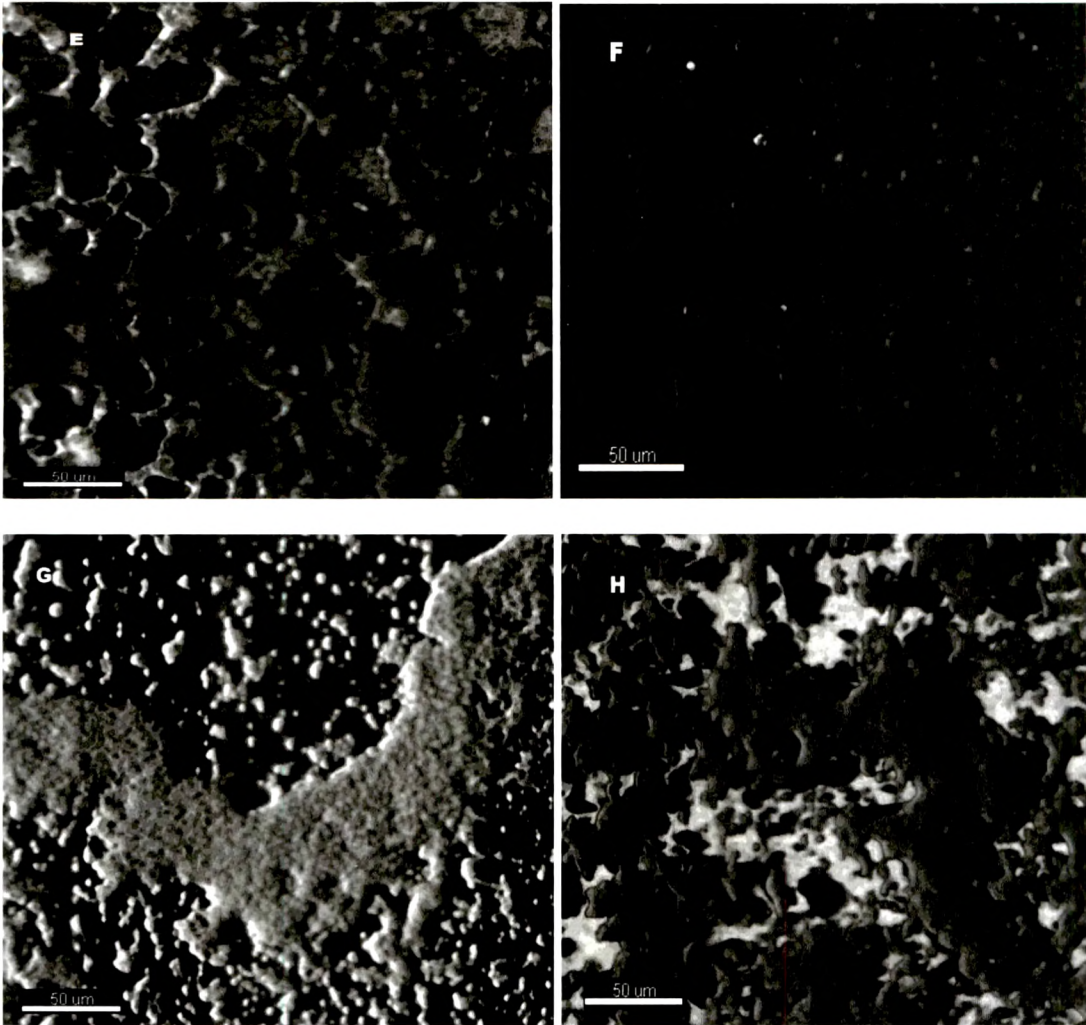
#### **3.3.4. $Ca^{++}$ and $Mg^{++}$ affect the biofilm architecture differentially**

Higher concentrations of calcium and magnesium were observed to increase biofilm formation. The mechanism for biofilm enhancement by  $Ca^{++}$  and  $Mg^{++}$  is possibly by inducing cohesion, which was found to be so in the *Paracoccus* sp. W1b biofilm as visualized by Environmental scanning electron micrographs (ESEM). Biofilm of aggregated

cells with distinct voids and a dense mass of biofilm cells were observed in the MM2 medium amended with 10mM MgSO<sub>4</sub>



continued.....



continued.....

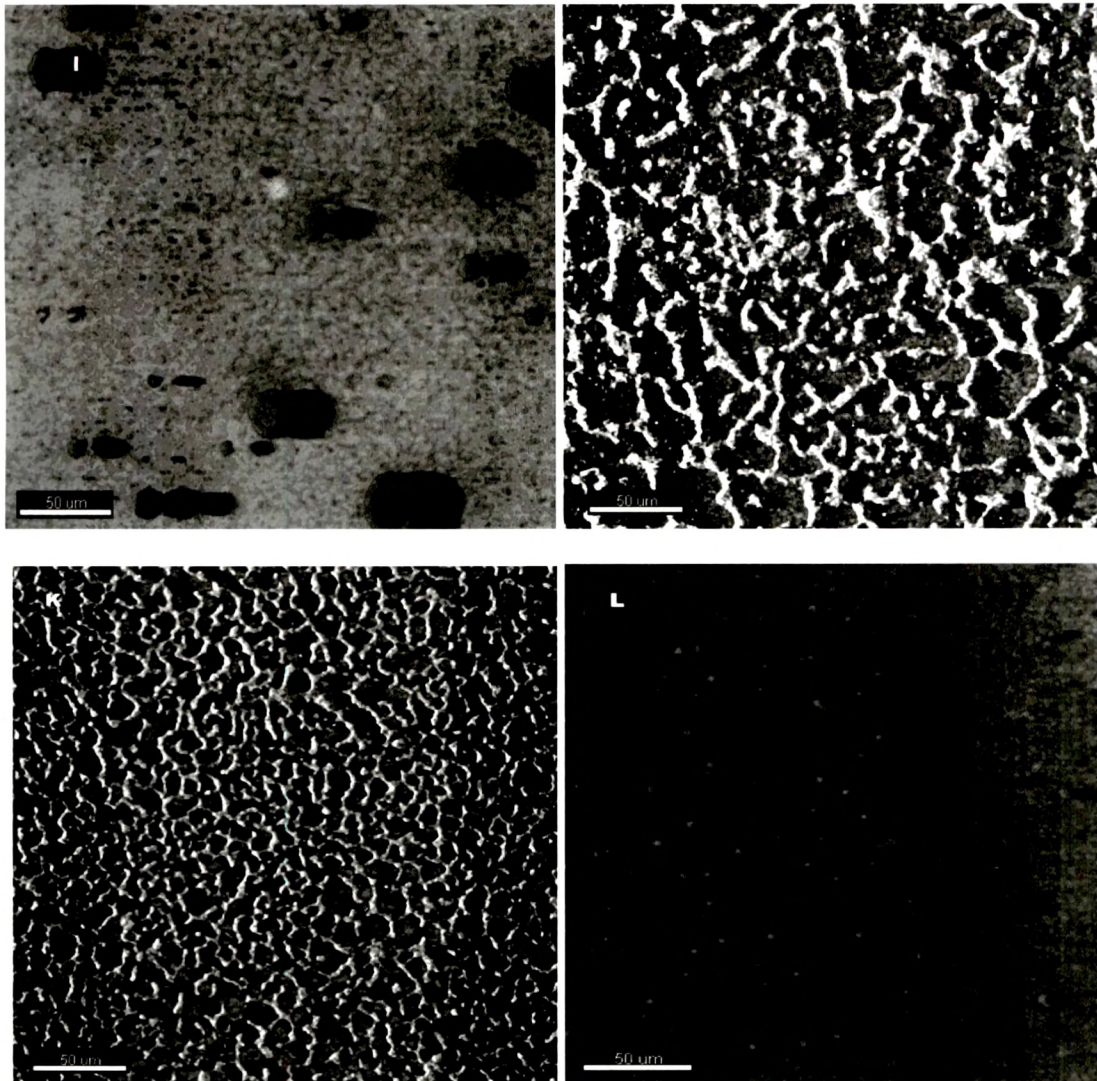


**Fig.3.5.** Representative CSLM images (40X magnification) of the *Paracoccus* sp. W1b biofilm structures formed in the twelve different media A-L of the Plackett-Burman experiment

**Table 3.3.** Structural parameters of biofilm formed in twelve different media of the Plackett-Burman experiment quantified from the CSLM images

Medium	Biomass ( $\mu\text{m}^3/\mu\text{m}^2$ )	Avg thickness ( $\mu\text{m}$ )	Roughness coefficient	Surface: bio- volume ( $\mu\text{m}^2/\mu\text{m}^3$ )	Max thickness ( $\mu\text{m}$ )	Substratum coverage
A	0.02±0.001	0.01±0.003	1.86±0.20	6.26±1.20	28.50±4.95	0.02±0.003
B	3.47±0.38	15.86±2.18	1.41±0.66	3.27±0.26	48.18±5.80	0.02±0.002
C	12.17±0.78	38.47±2.70	0.09±0.01	4.45±0.15	44.53±2.71	0.20±0.006
D	0.51±0.38	4.74±3.76	1.68±0.26	5.56±1.23	28.20±2.89	0.03±0.007
E	6.73±1.03	16.47±0.87	0.56±0.11	2.67±0.16	33.10±1.93	0.05±0.01
F	0.02±0.0005	0.006±0.001	1.99±0.0	6.95±0.01	29.63±2.26	0.02±0.0005
G	5.60±2.30	13.44±5.69	0.36±0.17	3.63±0.50	22.05±4.73	0.09±0.05
H	3.34±0.94	17.21±7.36	1.49±0.63	3.94±0.74	44.63±4.53	0.03±0.004
I	2.29±0.07	19.60±1.74	0.77±0.09	4.26±0.45	59.22±6.861	0.07±0.03
J	2.07±1.33	4.87±0.60	1.54±0.51	4.05±0.57	40.32±12.47	0.07±0.09
K	3.53±0.26	10.25±1.30	0.41±0.09	3.70±0.32	17.08±1.57	0.03±0.006
L	3.45±0.94	22.47±12.22	0.23±0.18	4.05±0.58	32.26±13.40	0.11±0.06

**Table 3.4.** Statistical analysis for influence of nutritional components on biofilm structural parameters from the results of Plackett-Burman design

Variable	KNO <sub>3</sub>		Sodium succinate		MgSO <sub>4</sub>		FeSO <sub>4</sub>		K <sub>2</sub> HPO <sub>4</sub>		CaCl <sub>2</sub>		MnCl <sub>2</sub>	
	E(Xi)	p-value	E(Xi)	p-value	E(Xi)	p-value	E(Xi)	p-value	E(Xi)	p-value	E(Xi)	p-value	E(Xi)	p-value
Biomass	1.78	0.1	-3.29	0.02	2.88	0.03	-1.09	0.26	-0.58	0.51	1.38	0.17	0.82	0.37
Avg thickness	5.76	0.51	-6.46	0.47	7.93	0.38	-7.78	0.39	-6.97	0.44	2.1	0.8	3.47	0.68
Roughness coefficient	-0.4	0.33	0.85	0.09	-0.47	0.27	0.45	0.28	0.02	0.94	0.4	0.33	0.03	0.92
Surface:Biovol	-0.05	0.72	0.31	0.09	-1.33	0.002	1.52	0.001	-0.43	0.04	0.38	0.06	0.57	0.02
Max thickness	0.72	0.8	11.73	0.02	9.52	0.03	-8.53	0.04	-12.24	0.01	4.9	0.16	5.98	0.11
Subs coverage	0.02	0.36	-0.04	0.11	0.02	0.29	-0.003	0.9	-0.04	0.11	-0.01	0.63	0.01	0.4

showed no such typical aggregations, however disconnected cells attached to the substratum were seen (Fig. 3.6 a). Cluster of cells were observed to be glued together in biofilms of high calcium and magnesium suggesting induction of cohesion by these cations.

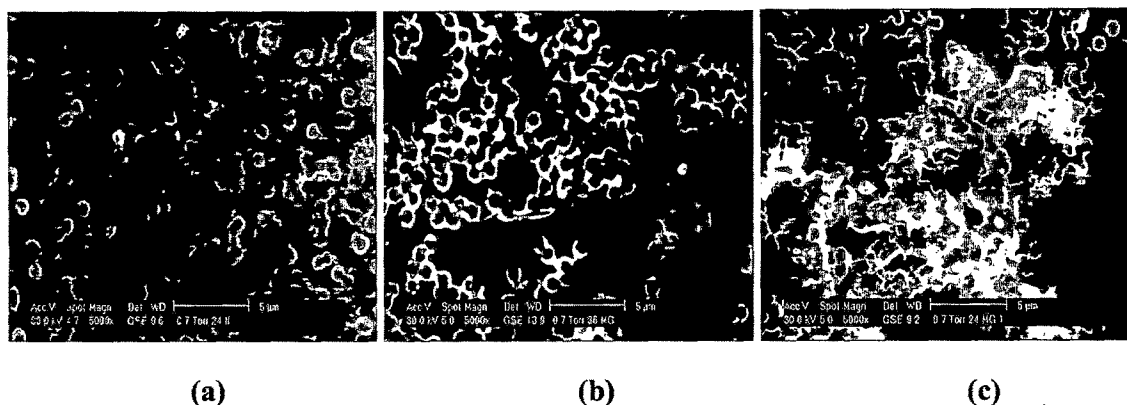


**Fig. 3.6.** ESEM images of the biofilm formed in (a) MM2 (b) MM2-Mg and (c) MM2-Ca medium

Further dissection of biofilm formed at high levels of  $\text{Ca}^{++}$  and  $\text{Mg}^{++}$  were done by analyzing their structures obtained from CSLM images. Although  $\text{Ca}^{++}$  and  $\text{Mg}^{++}$  enhanced biofilm growth by the same mechanism of inducing cohesion as visualized in ESEM micrographs (Figures 3.6 a-c), they affected surface to biovolume ratio differentially as observed from CSLM image analysis (Table 3.4). The E(Xi) values of biomass and thickness was positive for both the cations, but surface to volume ratio was negative in high magnesium media ( $P < 0.05$ ) and positive in high calcium media ( $p = 0.06$ ) (Table 3.4), suggesting that the overall architecture is affected differentially. To validate this observation, biofilm was allowed to form in MM2-Mg, MM2-Ca and control MM2 medium. MM2 - grown biofilm showed a well networked mosaic structure with distinct voids (Fig. 3.7a). Dense and confluent biofilm was observed in MM2-Ca (Fig. 3.7c), whereas monolayer cells with mosaic skeletal structure and dense protruding pillars of cell distributed over it was observed in MM2-Mg-grown biofilm (Fig. 3.7b). Biomass, average thickness, maximum thickness and substratum coverage was higher and roughness coefficient significantly lower in magnesium-induced biofilm as shown in Fig. 3.7d-h. In the calcium-induced biofilm, surface to biovolume ratio and roughness was significantly higher than the biofilm grown in MM2-Mg medium (Fig. 3.7) validating the earlier observation. Though the divalent cations, calcium and magnesium

are thought to be inducing the biofilm in similar way by crosslinking the cells and matrix, the overall architecture was found to be distinctly different. However, nitrate and phosphate showed no significant ( $p < 0.05$ ) changes in the biofilm structure. Significant

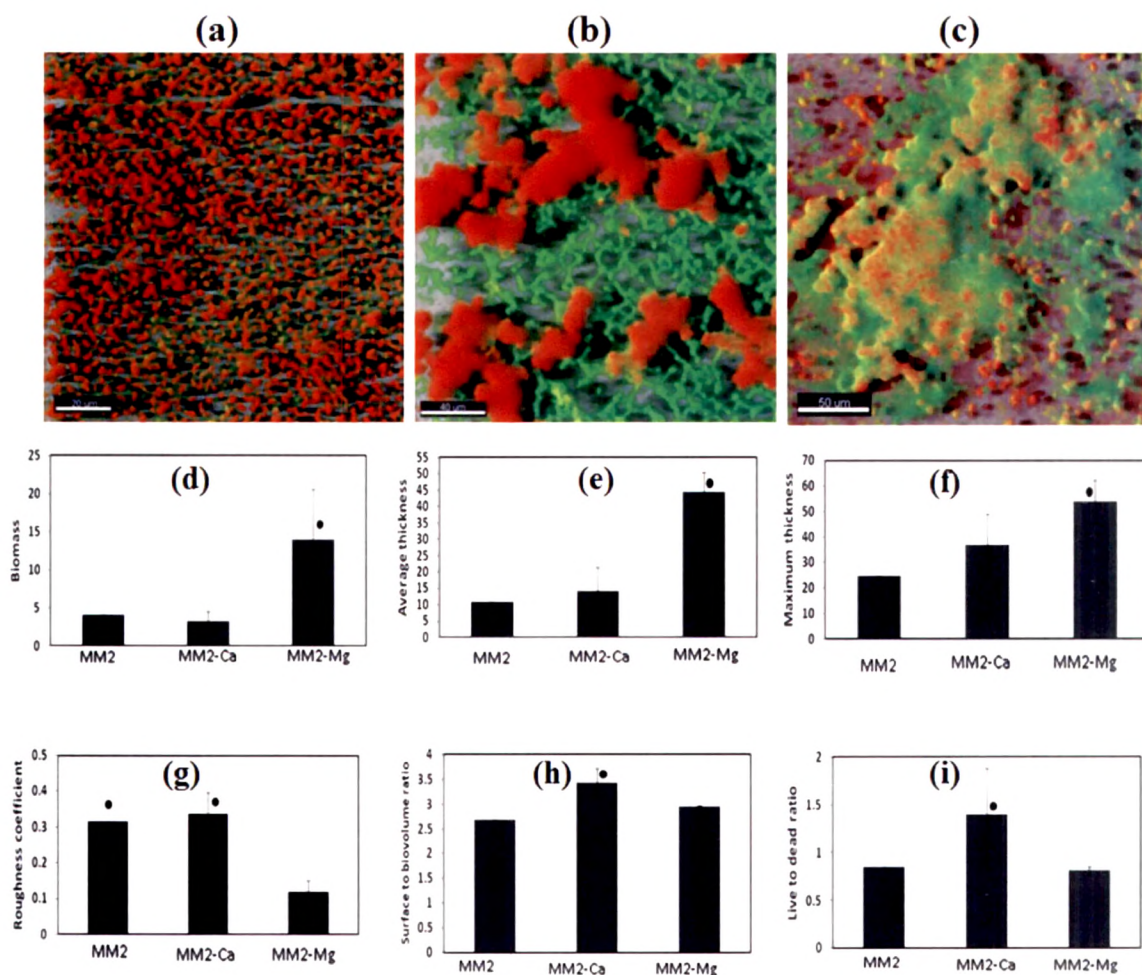


**Fig. 3.7.** Comparison of *Paracoccus* sp. W1b biofilm structures formed in MM2 medium, MM2-Mg and MM2-Ca respectively. CSLM images of biofilm (40X magnification) formed in (a) MM2 medium (b) MM2-Mg (c) MM2-Ca (d-i) COMSTAT results of various biofilm parameters from the CSLM images. One way ANOVA with Tukey test was used to determine significant differences. ● Indicates significance  $p < 0.05$

### 3.3.5. $\text{Ca}^{++}$ and $\text{Mg}^{++}$ - induced biofilm demonstrate enhanced denitrification activity

Denitrification activity was measured for the biofilms formed in MM2-Mg or MM2-Ca medium to correlate biofilm structure and denitrifying activity. Fig. 3.8 shows nitrate reduction to be significantly higher by the calcium and magnesium induced biofilm compared to biofilm grown in MM2 medium. It was 5.9 folds higher in MM2-Ca and 6.3 fold higher in MM2-Mg than MM2 grown biofilm. However, significant difference was not observed in nitrate reduction or nitrite accumulation between the biofilm formed in presence of high calcium and magnesium.

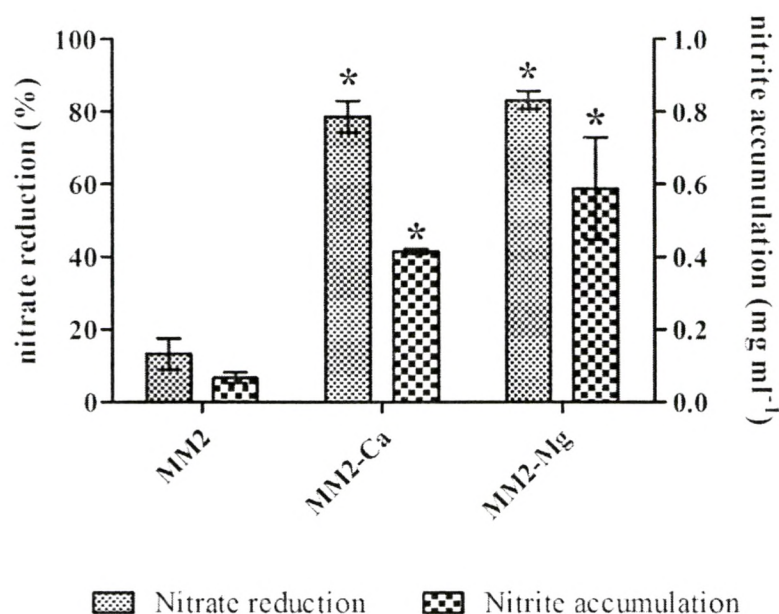


**Fig. 3.8.** Denitrification activity (six hours incubation) of the *Paracoccus* sp. W1b biofilm grown in MM2, MM2-Mg and MM2-Ca. Initial nitrate=3mM. Bars represent average values of atleast three independent experiments and error bars represent the standard deviations. One way ANOVA with Tukey test was used to determine significant differences.

\* Indicates significance  $p < 0.05$ .

### 3.3.6. Chelator treatment reveals importance of divalent cations in biofilm development

Role of divalent cations in biofilm formation by *Paracoccus* sp. W1b was further investigated by adding EDTA in the medium. An average of 1.56 fold reduction in biofilm formation was observed with every increase in EDTA concentration up to 0.5 mM (Fig. 3.9). Biofilm formation was completely inhibited at 1.0 and 10mM EDTA concentrations. Planktonic growth determined by enumerating CFU count was found to be  $10^{12}$  ml<sup>-1</sup> for EDTA in the range 0.0 - 0.5 mM, but its toxic effect was observed at concentrations above 0.5 mM. CFU counts of  $10^9$  ml<sup>-1</sup>,  $10^6$  ml<sup>-1</sup> and  $10^5$  ml<sup>-1</sup> were obtained with EDTA concentrations of 1.0, 5.0 and 10mM respectively.

Though biofilm formation decreased at increasing EDTA concentration, complete inhibition was not found at non-toxic EDTA concentrations. Hence, various ages of biofilm grown in MM2, MM2-Mg and MM2-Ca were treated with 10mM EDTA or EGTA (Fig. 3.11 a-c). Biomass in MM2 medium showed a reduction of 62% and 79% at the 6 hour and 12 hour old biofilm respectively after EDTA treatment and no reduction henceforth was observed as shown in

Fig. 3.11. When calcium-induced biofilm of various ages was treated with 10mM EGTA, 99% decrease was observed for biomass at 6 hour and 82% reduction at 12 hour period. Like the control MM2, further reduction was not found in biofilm on EGTA treatment at other time intervals, indicating that some divalent cations including calcium are significant in the initial stages of biofilm development possibly conferring structural stability by forming crosslinkages between cells or the matrix. Biofilm in 10mM magnesium showed reduction of biomass in the range 68% to 74%, although at 12 hour it showed 42% reduction. Pillar-like protruding cells of the biofilm were mainly found to get detached after EDTA treatment in high magnesium amended medium after 12 hour period (Fig. 3.12).

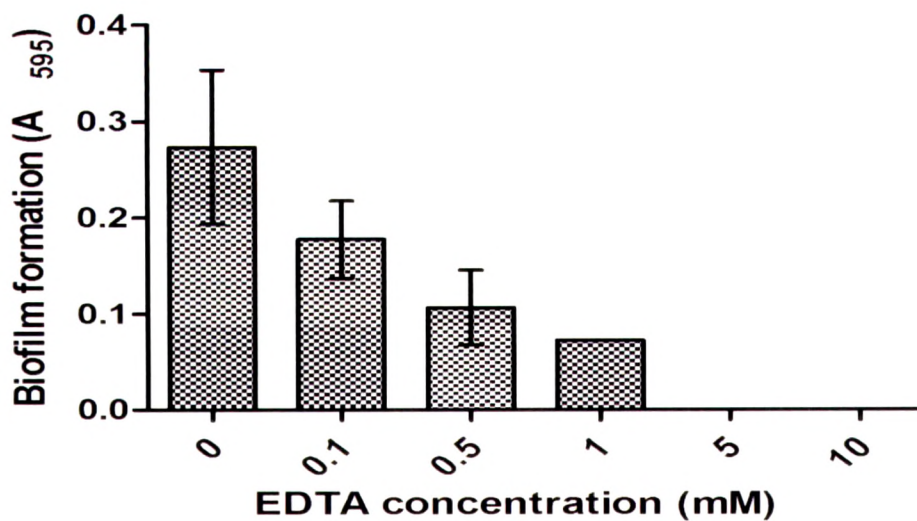


Fig.3.9. Effect of EDTA on *Paracoccus* sp. W1b biofilm formation.

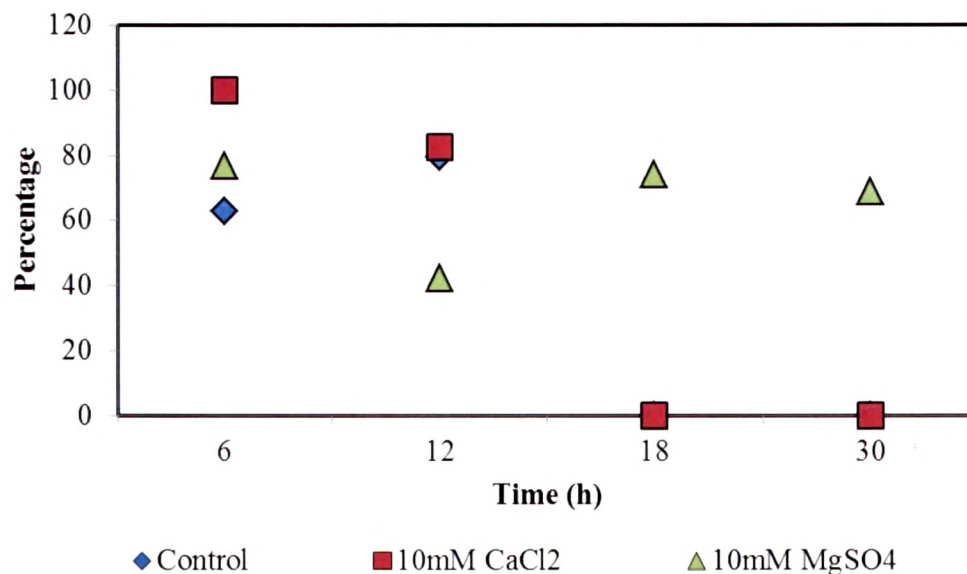
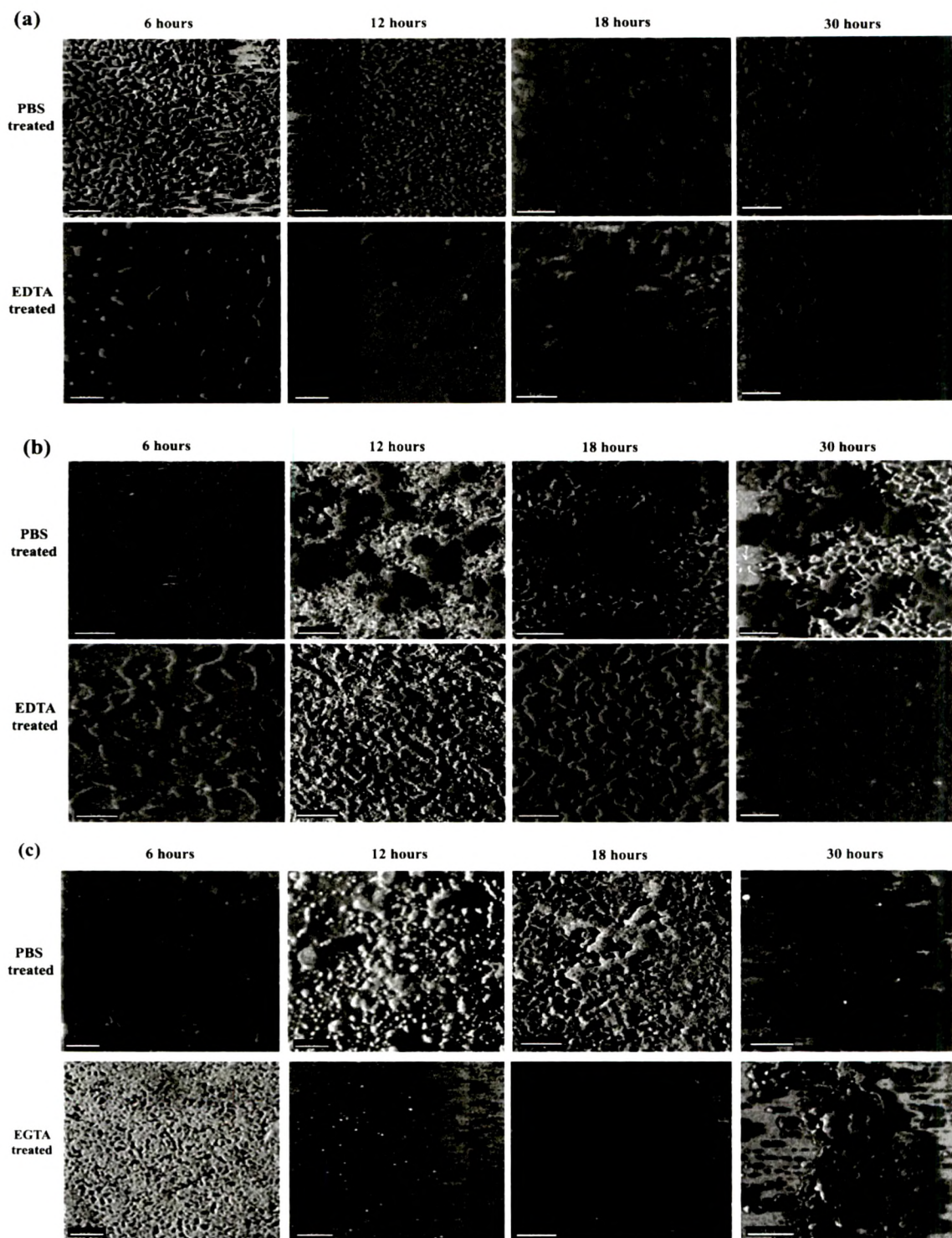
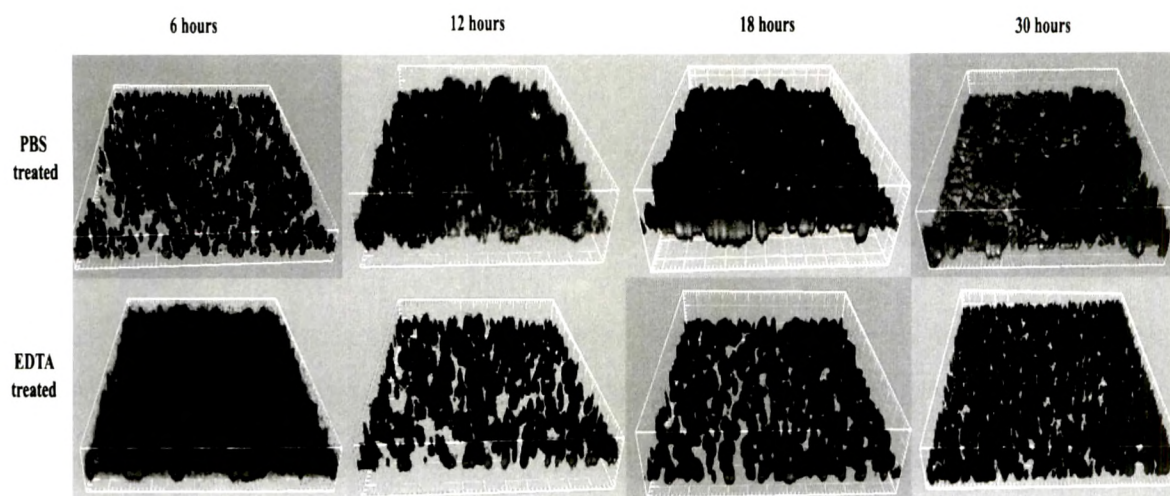


Fig.3.10. Percentage of biomass reduction at various ages of *Paracoccus* sp. W1b biofilm by EDTA/EGTA treatment quantified from the confocal images



**Fig. 3.11.** Representative confocal images of the chelator treated biofilm of various ages grown in (a) MM2 (b) MM2-Mg and (c) MM2-Ca medium.

(a)



(b)

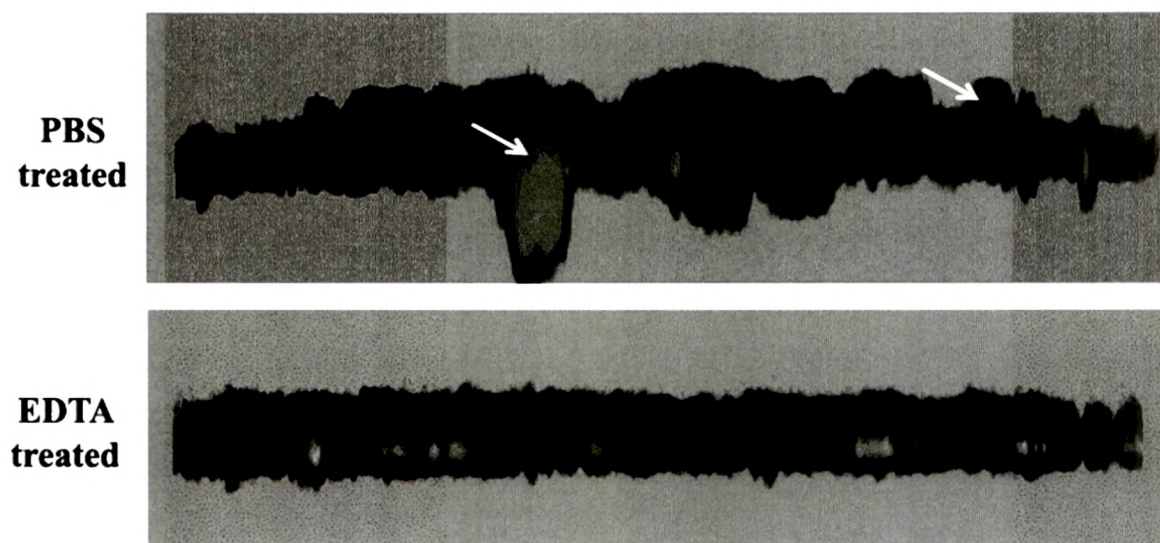


**Fig. 3.12.** Three dimensional image of variously aged biofilm grown in MM2-Mg medium before and after EDTA treatment (a) at different time points (b) the zoomed z-axis. The arrow mark indicates the representative subpopulations of pillar-like cells eluted after the EDTA treatment



### 3.3.7. Cell Surface Hydrophobicity decreases at higher magnesium concentration

Biofilm development takes place in various steps where the initial attachment stage is prominent. The cells attach to the abiotic surface by different molecular interactions like the hydrophobic, electrostatic, etc. Cell to cell interaction is important for further microcolony formation which also involves the molecular contacts. Magnesium ion had induced the biofilm formation in *Paracoccus* sp. W1b with a unique architecture and possible presence of subpopulations (Fig. 3.12). The cohesion of cells in the magnesium induced biofilm indicated electrostatic interactions to take place. However, the interaction in minimal magnesium concentration is not known. So the cell surface hydrophobicity was tested by the Bacterial Adhesion to Hydrocarbons (BATH) assay in minimal magnesium and high magnesium concentration in the medium. It was observed that the percent adherence to the hydrocarbons by the cells grown in the MM2 medium containing 1 mM MgSO<sub>4</sub> was 26.7%, while the percent adherence of the cells grown in MM2-Mg medium containing 10 mM MgSO<sub>4</sub> decreased to 10.6% (Fig. 3.13).

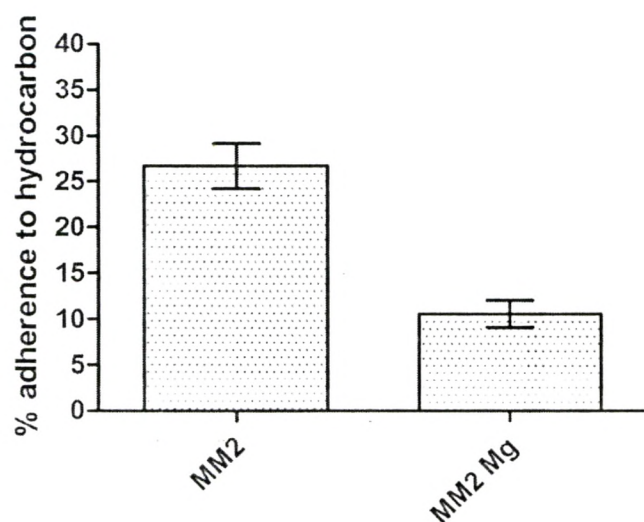


**Fig. 3.13.** Cell surface hydrophobicity of the *Paracoccus* sp. W1b cells as analyzed by the BATH assay. Error bars indicate the standard error where n=9.

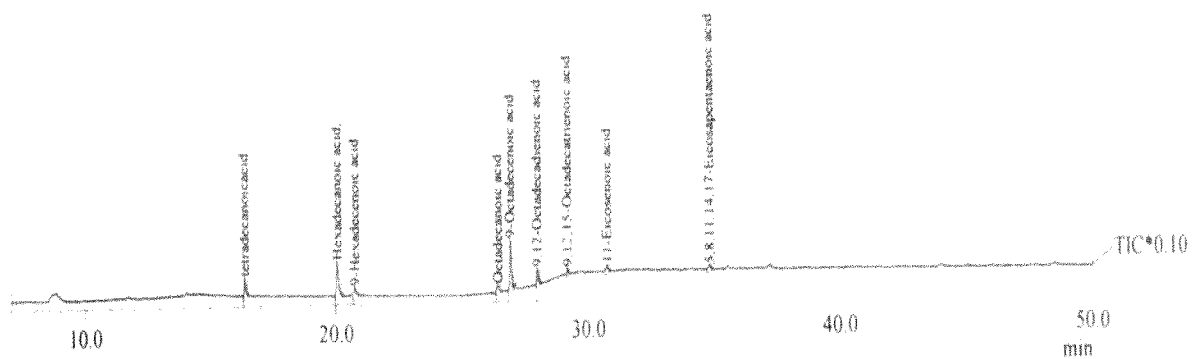
### 3.3.8. Composition of the cellular fatty acids differs among the subpopulations of *Paracoccus* sp W1b

In the previous experiments it was observed that the biofilm formed by *Paracoccus* sp. W1b in presence of 10 mM magnesium diversified into possible subpopulations with different structures, a thick pillar-like and a mosaic form (Fig. 3.12). When this biofilm was treated with EDTA, the pillar-like subpopulation detached from the biofilm leaving the mosaic form still adhered to the substratum. The two subpopulations were further separated by the EDTA treatment and FAME analysis was done to find the composition of the cellular fatty acids. It was observed that the mosaic form of subpopulation which still adheres to the substratum after EDTA treatment consisted of many different fatty acids with more of the unsaturated ones (Fig. 3.14 & Table 3.5), whereas the eluted pillar-like cells showed myristic, palmitic and the 9-octadecanoic acids. The significant qualitative changes in the fatty acids confirm the presence of subpopulation in the magnesium-induced biofilm of *Paracoccus* sp. W1b

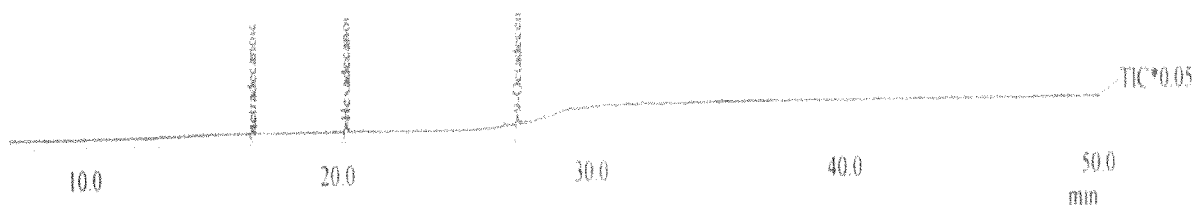
### 3.3.9. Influence of the nitrogenous oxides on *Paracoccus* sp. W1b biofilm

The higher or the lower concentration of the nitrate did not affect the biofilm formation significantly as seen in the Plackett-Burman experiment. Denitrification involves different nitrogenous oxide intermediates where nitrite and nitric oxide are toxic to the cells (Poole 2005). Hence the influence of nitrite and nitric oxide on the biofilm formation was tested in this experiment, where the different nitrite concentrations showed no significant effect on the biofilm formation of *Paracoccus* sp. W1b (Fig 3.15). Production of nitric oxide was done by using nitroprusside where 10 and 25  $\mu\text{M}$  showed a significant reduction in the biofilm formation by *Paracoccus* sp. W1b (Fig 3.16). However the nitric oxide generated by nitroprusside did not show any significant effect on the formed biofilm of various ages (Fig 3.17).

(a)



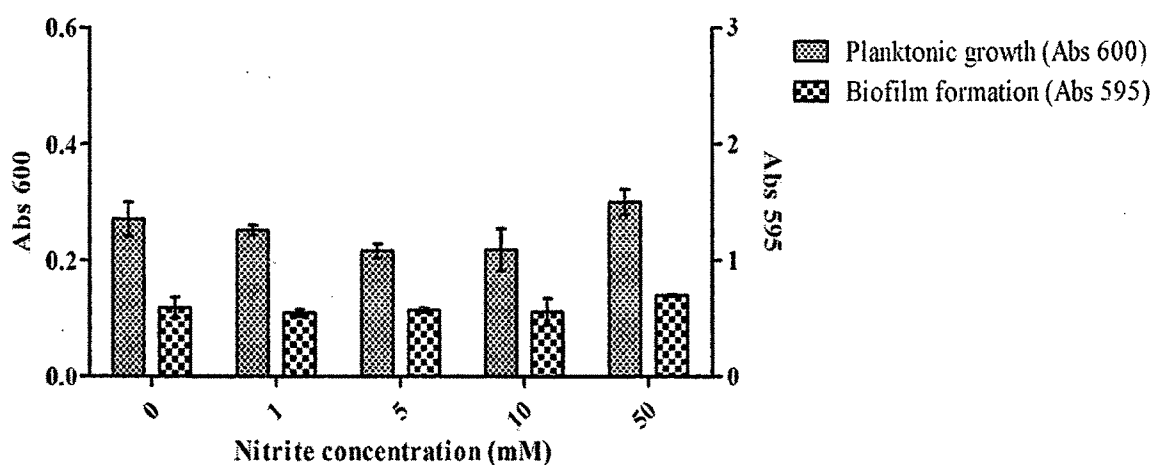
(b)



**Fig. 3.14.** FAME results of biofilm subpopulations grown in MM2-Mg medium after EDTA treatment (a) The mosaic-layered cells adhered to the substratum (b) The pillar-like eluted cells

**Table 3.5.** The cellular fatty acids analyzed by FAME

Sample	Fatty acids present
Mosaic layered biofilm cells adhered to the surface after EDTA treatment in MM2-Mg medium	Tetradecanoic acid
	Hexadecanoic acid
	9-Hexadecenoic acid
	Octadecanoic acid
	9-Octadecanoic acid
	9, 12-Octadecadienoic acid
	9, 12, 15-Octadecatrienoic acid
	11-Eicosenoic acid
5,8,11,14,17-Eicosapentaenoic acid	
Pillar-like eluted biofilm cells after EDTA treatment in MM2-Mg medium	Tetradecanoic acid
	Hexadecanoic acid
	9-Octadecanoic acid

**Fig. 3.15.** Biofilm formation by *Paracoccus* sp. W1b in presence of different nitrite concentrations. Error bars indicate SD

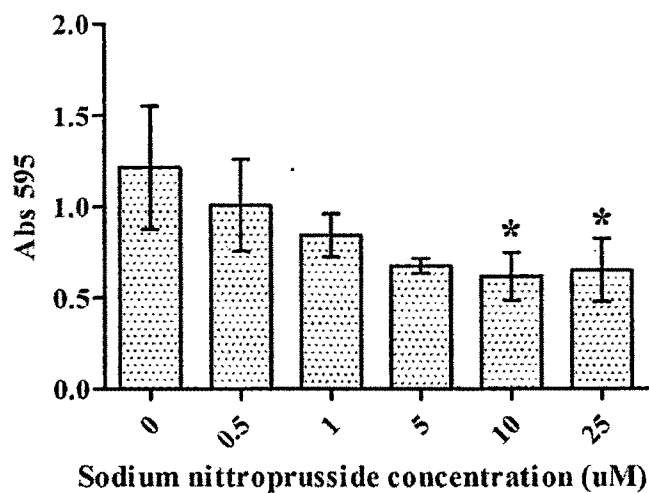


**Fig. 3.16.** Influence of nitric oxide produced by different nitroprusside concentrations on the formation of *Paracoccus* sp. W1b biofilm. Error bars indicate SD. One way ANOVA with Tukey's test was used to determine significant differences. \* = Significant at  $p < 0.05$

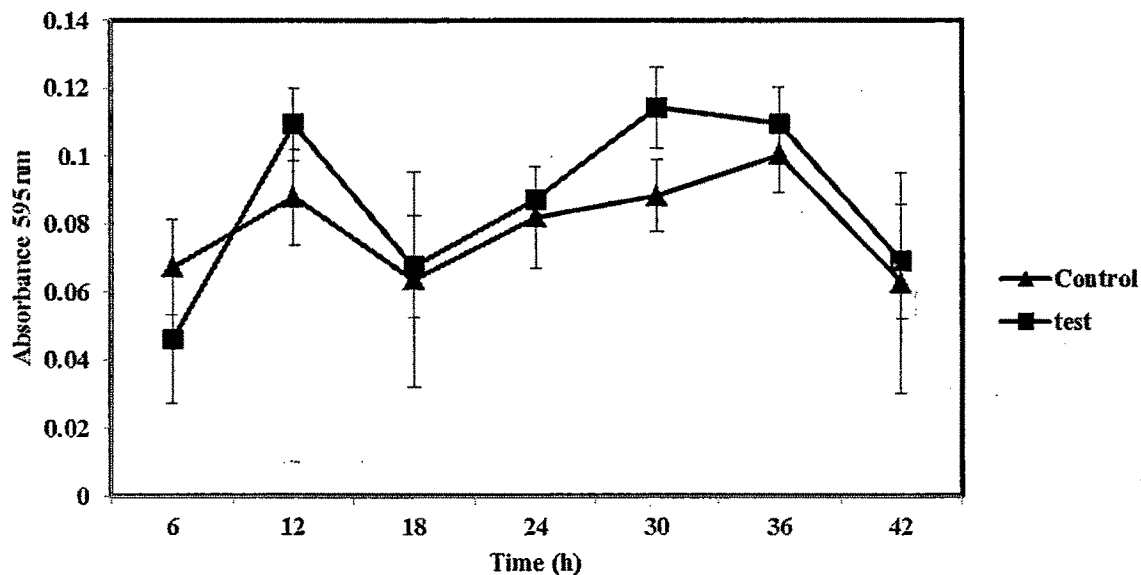


**Fig. 3.17.** Influence of nitric oxide on different ages of the *Paracoccus* sp. W1b biofilm. Control = PBS treated and Test = Nitric oxide treated

### 3.4. Discussion

In the previous chapter, *Paracoccus* sp. W1b was found to be an efficient denitrifier which could also tolerate and reduce the nitrogenous oxides at high nitrate concentrations. Biofilm formation and the influence of different chemical factors on the architecture of the biofilm of this isolate were investigated in this study. Biofilm formation of the isolate was confirmed by the brightfield microscopic analysis and ESEM, which showed clusters of coccoid cells adhered to the polystyrene surface (Fig. 3.1 & 3.2). In order to investigate the influence of nutrients on biofilm formation of *Paracoccus* sp. W1b, statistical design of experiment by microtiter plate assay was adopted. Microtiter plate assay utilizes crystal violet stain, which binds to negatively charged molecules in the cell surface including EPS with acidic residues, thus quantifying the overall biomass which is the measure of biofilm formed. The divalent cations, magnesium, calcium and manganese increased biofilm formation at higher concentrations, whereas iron inhibited biofilm formation at its higher concentration (Fig. 3.3). Increasing succinate concentration in the MM2 medium increased the biofilm formation relatively (Fig. 3.3). However, the biofilm formed in presence of higher magnesium concentration was more than the other nutrients. A high throughput statistical methodology was further adapted to see the effects of the nutrient concentrations on the biofilm formation and its architecture.

Influence of nutrient parameters on biofilm formation was observed to be distinct in twelve different media by either inducing or repressing biofilm formation (Fig. 3.4b).  $E(X_i)$  values based on the assay showed significant increase in biofilm formation affected by succinate, magnesium, calcium and manganese, whereas iron repressed biofilm formation at higher concentrations (Fig. 3.4). Biofilm architecture, as affected by various nutrients was determined by combining the different structural parameters quantified from confocal images. Fluorescent nucleic acid stains, i.e., SYTO9 and propidium iodide were used to stain biofilm for confocal microscopy and their images were used to quantify the structural parameters including biomass by the COMSTAT program. All nutrient components used, showed to significantly or nearly significantly affect every biofilm structural parameter tested, except average thickness, emphasizing the importance of their concentrations on

modulating biofilm structures (Table 3.4). Adaptation of biofilm structures according to changes in local substrate concentrations has also been demonstrated by computational models (Wimpenny & Colasanti, 1997).

High succinate concentrations affected the biofilm formation positively as shown by microtiter plate assay (Fig. 3.4) whereas image analysis showed higher concentration of succinate to affect biomass negatively, but maximum thickness, roughness coefficient, surface to volume ratio and live to dead ratio positively (Table 3.4). Microtiter plate assay gives the intensity value of crystal violet as the overall biomass in the biofilm, whereas the COMSTAT analysis of the image reflects the amount of biomass (fluorescent intensity of stained nucleic acids) excluding exopolysaccharides or proteins in the biofilm. The disparity between the microtitre plate and confocal image analysis may be due to the increased production of exopolysaccharides at higher concentration of succinate. Enhanced synthesis of EPS due to availability of excess carbon source has also been discussed in a review on biofilm exopolysaccharides by Sutherland (2001).

Iron showed negative  $E(X_i)$  values for biomass ( $p=0.26$ ) and maximum thickness ( $p=0.04$ ) implying a positive influence on these parameters at lower concentration (Table 3.4). Planktonic growth was not significantly affected by higher iron concentrations (Fig. 3.4) indicating that the higher concentrations used were not toxic on growth. Reduction in biofilm formation at increasing iron concentrations has been reported for *P. aeruginosa* (Musk et al. 2005; Yang et al. 2007) and *S. epidermidis* strains (Johnson et al. 2005). Reduction in biofilm biomass and thickness at high levels of iron was also observed by Yang et al. (2007). However, importance of minimal amounts of iron in biofilm development is demonstrated by Singh et al. (2002) and Banin et al. (2005). Deighton & Borland (1993) showed increased slime production in iron-limited conditions for *S. epidermidis* strains known to form biofilms encased with slime on prosthetic medical devices. Yang et al. (2007) observed decrease in extracellular DNA with increasing iron concentrations and also discussed their unpublished result where lower levels of iron induced higher production of extracellular DNA. Thus, it illustrates that lower levels of iron is necessary for biofilm formation, whereas excess iron represses biofilm formation.

Divalent cations other than iron, like calcium, magnesium and manganese showed a positive effect on biofilm formation in microtiter plate assay significantly at higher concentrations (Fig. 3.4). Many reports have demonstrated the involvement of calcium in biofilm formation. Kierek & Watnick (2003), showed the important role of O-antigen in calcium-dependent biofilm formation of *V. cholerae*. Calcium addition enhanced biofilm thickness by nearly 20-fold in mucoid *P. aeruginosa* biofilms (Sarsikova et al. 2005). Magnesium is also known to enhance biofilm formation. Adhesion of *S. epidermidis* increased two to four fold with addition of magnesium and calcium to plastic (Dunne & Burd, 1992). Song & Leff (2006) observed increase in bacterial attachment with increasing magnesium concentrations. Plackett-Burman statistical experiment showed calcium and magnesium to positively affect biomass and maximum thickness of *Paracoccus* sp. W1b biofilm (Table 3.4). Tanji et al. (1999) had indicated that the thickness of biofilm increased due to increase in density of dead cells in the biofilm. Thus, live to dead ratio of cells was also calculated and significant increase in live cell fraction was found with the biofilm grown in MM2-Ca medium and no significant difference was observed between MM2 and the MM2-Mg grown biofilms (Fig. 3.7i) suggesting, that the accumulation of dead cells is not a rationale for increase in the thickness of *Paracoccus* sp. W1b biofilm.

Chen and Stewart (2002) observed reduction in apparent viscosity of *P. aeruginosa* biofilm cells with magnesium and calcium, whereas the viscosity increased with iron salts. Contrary to this observation, ESEM visualization of *Paracoccus* sp. W1b biofilm indicated cohesion of cells induced by magnesium and calcium (Fig. 3.6a-c), thus enhancing biofilm formation, whereas repression of biofilm formation was observed by iron at higher concentrations (Fig. 3.4 & Table 3.4). However, contrast in biofilm structures was observed for the biofilm formed at high level of calcium and magnesium in results provided by CSLM. Magnesium affected surface to volume ratio negatively, whereas calcium positively (Table 3.4). Negative surface to volume implies lesser fraction of cells exposed towards bulk liquid phase. Increased biomass with low surface to volume ratio indicates clustering of cells into tall pillars, which allows fewer fraction of cells exposed to surface, but converse is true for positive surface to volume ratio. Contrasting biofilm structures were formed, though both are thought to contribute cohesion by crosslinking the cells and matrix in the same way. Lattner

et al. (2003) demonstrated differential affinity of magnesium and calcium to alginate, a major EPS produced by *P.aeruginosa* biofilm. This disparity is possible because of the difference in their orbital structure, binding strength, and the rate constant of binding to the cell surface or matrix molecules (Geesey et al. 2000). Klausen et al. (2006) have proposed that the natural selection of different biofilm subpopulations in response to environmental conditions is the underlying reason for structural differences in *P.aeruginosa* biofilms grown in presence of citrate or glucose. Similarly in this study with *Paracoccus* sp. W1b, high level of magnesium and calcium possibly promoted the formation of protruding sub-population of cells at different frequencies contributing to difference in biofilm architecture.

Wimpenny & Colasanti (1997) reviewed three different conceptual models of biofilm structures, the water-channel, heterogenous mosaic and a dense biofilm model. Comparisons could be drawn here to these models with *Paracoccus* sp. W1b biofilm. A typical mosaic form of biofilm cells with distinct voids was observed in the biofilm grown in control MM2 medium (Fig. 3.7a) similar to the water-channel model. We also observe some parallels of magnesium-induced biofilm (Fig. 3.7b) with the heterogenous mosaic model and calcium-induced biofilm (Fig. 3.7c) with dense biofilm model. Magnesium-induced biofilm of *Paracoccus* sp. W1b showed pillar-like protrusions of cell clusters distributed on a monolayer mosaic kind of networked cells (Fig. 3.7b). In heterogenous mosaic model, well separated stacks of microcolonies are attached to substratum with small bottom layer of cells in the background. This kind of biofilm structure was described on natural biofilm in water distribution systems. Calcium-induced biofilm of *Paracoccus* sp. W1b formed dense, confluent aggregation of cells (Fig. 3.7c). Dental plaque biofilms complies with the dense biofilm model (Wimpenny & Colasanti, 1997). Saliva-derived components are also known to have high calcium ions (García-Godoy & Hicks, 2008) and aggregation of cells induced by calcium in a cariogenic strain of *S. downei* has been demonstrated by Rose (2000).

Addition of EDTA in the medium decreased the amount of biofilm formation of *Paracoccus* sp. W1b (Fig. 3.9) indicating the role of divalent cations in biofilm development. Turakhia et al. (1983) treated the biofilm with EGTA causing it to detach, signifying the role of calcium in clasping the cells together. Reduction in adhesion of *S.epidermidis* cells by EDTA

treatment was observed by Dunne & Burd (1992). Decrease in apparent viscosity on EDTA treatment (Chen and Stewart, 2002) and loss of biofilm cells by addition of EDTA was also found in *P.aeruginosa* cells (Banin et al. 2006). Though there is reduction, complete inhibition of biofilm formation was not observed in any of these studies. Hence, biofilm of various ages were treated with the chelator in this study to examine the role of divalent cations during biofilm development. Biofilm in MM2 and MM2-Ca media showed no reduction in biomass after 12 hour period with chelator treatment (Fig. 3.10 and 3.11 a & c). This suggests that the divalent cations are necessary in the initial stages of the biofilm development. Nutrients like phosphate and iron are also implicated in microcolony and maturation stages respectively during biofilm development (Monds et al. 2007; Banin et al. 2005). On the other hand, increased biomass reduction with progression in time was observed for the biofilm grown in MM2-Mg medium treated with EDTA (Fig. 3.10 & 3.11 b). Availability of higher magnesium concentration has been possibly exploited by a subpopulation of *Paracoccus* sp. W1b even at later stages of development, due to which they are susceptible to the EDTA treatment. It was also observed that the protruding pillar-like cells were more susceptible to EDTA than the basal mosaic layer of cells in 10mM magnesium amended medium (Fig. 3.11 & 3.12), indicating that the pillar-like cells are held together possibly by magnesium ions. This indicates that protruding cells are possibly subpopulations naturally selected by high level of magnesium unlike the basal mosaic layer.

BATH assay showed that the cells grown in MM2-Mg medium had cell surface hydrophobicity 1.5 folds lower from those of the MM2 medium grown cells (Fig. 3.13). This shows that the cells grown in higher magnesium concentration adapts by exploiting the magnesium ions for crosslinking between cell to cell and decreasing their hydrophobic property. It can also be speculated that the mosaic layered cells of the biofilm grown in MM2-Mg medium might have more cell surface hydrophobicity than the pillar-like cells because the EDTA treatment caused dispersal of the latter (Fig. 3.12), where electrostatic interaction might be dominated in these pillar-like cells. Further these two structurally different cells were separated by the EDTA treatment from the biofilm grown in MM2-Mg medium and the cell fatty acid profiles investigated by FAME analysis. It was observed that the mosaic-layered cells still adhered to the substratum surface after the EDTA treatment

consisted of more unsaturated fatty acids including mono, di, tri and penta unsaturated fatty acids, while the pillar-like cells consisted of only tetra, hexa and 9-octadecanoic acids (Fig. 3.14 & Table 3.5). The different fatty acids profile confirms the presence of subpopulation. Changes in the fatty acid composition due to change in temperature, osmolarity, pH and other nutrients are reported in different organisms (O'Leary 1962). The two component system, phoP-phoQ in *Salmonella typhimurium* senses the magnesium concentration in the environment and modifies the lipid-A which also helps in resistance to cationic peptides (Guo et al. 1997), while *Pseudomonas aeruginosa* has altered lipid-A structures in cystic fibrosis infections (Ernst et al. 1999).

High nitrate levels did not show a significant effect on biofilm formation as observed by microtiter plate assay (Fig. 3.4b), however it had a positive influence on biomass ( $p=0.109$ ) as analyzed from CSLM images (Table 3.4). Other biofilm parameters were not significantly influenced by altered nitrate levels (Table 3.4). Activation of denitrification pathway requires not only presence of nitrate but also oxygen-limiting conditions (Tiedje, 1994). Denitrification activity was significantly high in MM2-Ca and MM2-Mg than MM2 biofilm of *Paracoccus* sp. W1b (Fig. 3.8). Decreasing dissolved oxygen (DO) concentrations from bulk fluid phase into the microcolony was observed in dense biofilm, but significant levels of DO was seen in less dense microcolony by Costerton et al. (1995). Biofilm grown in MM2-Ca and MM2-Mg formed thick biofilms with high biomass compared to the biofilm grown in MM2 medium (Fig. 3.7), suggesting that the reduced DO concentration is the possible reason for inducing more denitrification activity. However, denitrification was not significantly different between MM2-Ca and MM2-Mg biofilms (Fig. 3.8). Nitrite, an intermediate of denitrification is shown to inhibit *Staphylococcus aureus* biofilm formation (Schlag et al. 2007) and nitric oxide has been implicated in the dispersal of *P.aeruginosa* biofilm (Barraud et al. 2006). However, different nitrite concentrations showed no effect on the biofilm formation of *Paracoccus* sp. W1b (Fig. 3.15), and nitric oxide also was not observed to cause dispersal of the formed biofilm (Fig. 3.17).

It was thus observed that the nutrients can significantly impact the biofilm formation including their architecture. However, *Paracoccus* sp. W1b biofilms were not affected

significantly by the tested nitrogenous oxides in contrast to other organisms. On the other hand, the results obtained for *Paracoccus* sp. W1b biofilm also seems apparent for the ecological adaptation model proposed by Klausen et al. (2006).

### 3.5. References

- Akolkar A, Bharambe N, Trivedi S and Desai A. 2008. Statistical optimization of medium components for extracellular protease production by an extreme haloarchaeon, *Halobacterium* sp. SP1(1). *Lett Appl Microbiol.* 48: 77-83
- Baker C. S, Ferguson S. J, Ludwig Bernd, Page M. D, Richter O-M. H, Van Spanning Rob J. M. 1998. Molecular genetics of the genus *Paracoccus*: Metabolically versatile bacteria with bioenergetic flexibility. *Microbiol Mol Bio Rev.* 62:1046-1078
- Banin E, Brady KM, Greenberg EP. 2006. Chelator-induced dispersal and killing of *Pseudomonas aeruginosa* cells in a biofilm. *Appl Env Microbiol.* 72:2064–2069.
- Banin E, Vasil ML, Greenberg EP (2005): Iron and *Pseudomonas aeruginosa* biofilm formation  
*Proc Nat Acad Sci.* 102:11076–11081.
- Barraud N, Hassett D. J, Hwang S-H, Rice S. A, Kjelleberg S, Webb J. S. 2006. Involvement of nitric oxide in biofilm dispersal of *Pseudomonas aeruginosa*. *J Bacteriol* 188:7344-7353
- Chen X, Stewart PS. 2002. Role of electrostatic interactions in cohesion of bacterial biofilms. *Appl Microbiol Biotechnol.* 59:718-720.
- Costerton JW, Lewandowski Z, Caldwell DE, Korber DR, Lappin-Scott HM. 1995. Microbial biofilms. *Annu Rev Microbiol.* 49:711-745.
- Deighton M, Borland R. 1993. Regulation of slime production in *Staphylococcus epidermidis* by iron limitation. *Infect Immun.* 61:4473-4479.
- Dunne WM, Burd EM. 1992. The effects of magnesium, calcium, EDTA and pH on the *In Vitro* adhesion of *Staphylococcus epidermidis* to plastic. *Microbiol Immun.* 36:1019-1027.

- Ernst, R.K., Yi, E.C., Guo, L., Lim, K.B., Burns, J.L., Hackett, M., Miller, S.I., 1999, Specific lipopolysaccharide found in cystic fibrosis airway *Pseudomonas aeruginosa*. *Science*. 286, 1561-1565.
- García-Godoy F, Hicks MJ. 2008. Maintaining the integrity of the enamel surface: The role of dental biofilm, saliva and preventive agents in enamel demineralization and remineralization. *J Am Dent Assoc*. 139:25S-34S.
- Geesey GG, Wigglesworth-Cooksey B, Cooksey KE. 2000. Influence of calcium and other cations on surface adhesion of bacteria and diatoms: A review. *Biofouling*. 15:195-205.
- Gohel V, Chaudhary T, Vyas P, Chhatpar HS. 2006. Statistical screenings of medium components for the production of chitinase by the marine isolate *Pantoea dispersa*. *Biochem Eng J*. 28:50-56.
- Guo, L., Lim, K.B., Gunn, J.S., Bainbridge, B., Darveau, R.P., Hackett, M., Miller, S.I., 1997, Regulation of lipid A modifications by *Salmonella typhimurium* virulence genes phoP-phoQ. *Science*. 276, 250-253.
- Heydorn A, Nielsen AT, Hentzer M, Sternberg C, Givskov M, Ersboll BK, Molin, S. 2000 Quantification of biofilm structures by the novel computer program COMSTAT. *Microbiology*. 146:2395-2407.
- Johnson M, Cockayne A, Williams PH, Morrissey JA. 2005. Iron-responsive regulation of biofilm formation in *Staphylococcus aureus* involves Fur-dependent and Fur-independent mechanisms. *J Bacteriol*. 187:8211-8215.
- Kierek K, Watnick PI. 2003. The *Vibrio cholerae* O139 O-antigen polysaccharide is essential for Ca<sup>2+</sup>-dependent biofilm development in sea water. *Proc Nat Acad Sci*. 100:14357-14362.
- Kim, I.S., Jang, A., Ivanov, V., Stabnikova, O., Ulanov, M., 2004, Denitrification of Drinking Water Using Biofilms Formed by *Paracoccus denitrificans* and Microbial Adhesion. *Env Eng Sci*. 21, 283-290.
- Klausen M, Gjermansen M, Kreft JU, Tolker-Nielsen T. 2006. Dynamics of development and dispersal in sessile microbial communities: examples from *Pseudomonas aeruginosa* and *Pseudomonas putida* model biofilms. *FEMS Microbiol Lett*. 261:1-11.

- Lattner D, Flemming HC, Mayer C. 2003.  $^{13}\text{C}$ -NMR study of the interaction of bacterial alginate with bivalent cations. *Int J Biol Macromol.* 33:81-88.
- Moller S, Korber DR, Wolfaard GM, Molin S, Caldwell DE. 1997. Impact of nutrient composition on a degradative biofilm community. *Appl Env Microbiol* 63:2432–2438.
- Monds RD, Newell PD, Gross RH, O'Toole GA. 2007. Phosphate-dependent modulation of c-di-GMP levels regulates *Pseudomonas fluorescens* Pf0-1 biofilm formation by controlling secretion of the adhesin LapA. *Mol Microbiol.* 63:656-679.
- Montgomery DC. 1997. In Design and analysis of experiments. fourth ed, Wiley, New York
- Musk DJ, Banko DA, Hergenrother PJ. 2005. Iron salts perturb biofilm formation and disrupt existing biofilms of *Pseudomonas aeruginosa*. *Chem Biol.* 12:789-796.
- Neef, A., Zaglauer, A., Meier, H., Amann, R., Lemeer, H., Schleifer, K.-H., 1996, Population analysis in a denitrifying sand filter: conventional and in situ Identification of *Paracoccus* spp. in methanol-fed biofilms. *Appl Env Microbiol.* 62, 4329–4339.
- O'Leary, W.M., 1962, The fatty acids of bacteria. *Bacteriol Rev.* 26, 421-447.
- O'Toole G, Kaplan H. B, and Kolter R. 2000. Biofilm formation as microbial development. *Ann Rev Microbiol.* 54: 49-79
- Peng Xiang, Zhang J S., Li Y Y., Li Wen, Xu G M., Yan C. Y. 2008. Biodegradation of insecticide carbofuran by *Paracoccus* sp. YM3. *J Env Sci Health.* Part B. 43: 588-594
- Plackett RL, Burman JP. 1946. The design of optimum multifactorial experiments. *Biometrika.* 33:305-325.
- Poole, R.K., 2005, Nitric oxide and nitrosative stress tolerance in bacteria. *Biochem Soc Transac.* 33, 176-180.
- Prakash B, Veeregowda BM, Krishnappa G. 2003. Biofilms: A survival strategy of bacteria. *Curr Sci.* 85:1299-1307.
- Priester JH, Horst AM, Werfhorst LCVD, Saleta JL, Mertes LAK, Holden PA. 2007. Enhanced visualization of microbial biofilms by staining and environmental scanning electron microscopy. *J Microbiol Meth.* 68:577–587.
- Rose RK. 2000. The role of calcium in oral streptococcal aggregation and the implications for biofilm formation and retention. *Biochimica et Biophysica Acta.* 1475:76-82.

- Sarsikova S, Patrauchan MA, Berglund D, Nivens DE, Franklin MJ. 2005. Calcium-induced virulence factors associated with the extracellular matrix of mucoid *Pseudomonas aeruginosa* biofilms. *J Bacteriol.* 187:4327-4337.
- Sauer K, Cullen MC, Rickard AH, Zeef LAH, Davies DG, Gilbert P. 2004. Characterization of nutrient-induced dispersion in *Pseudomonas aeruginosa* PAO1 biofilm. *J Bacteriol.* 186:7312-7326.
- Schlag S, Nerz C, Birkenstock TA, Altenberend F, Götz F (2007): Inhibition of Staphylococcal biofilm formation by Nitrite. *J Bacteriol.* 189:7911-7919.
- Siller H, Rainey F A., Stackebrandt E, and Winter J. 1996. Isolation and Characterization of a new Gram-negative, acetone-degrading, nitrate-reducing bacterium from soil, *Paracoccus solventivorans* sp. nov. *Int J Sys Bac.* 46: 1125-1130
- Singh PK, Parsek MR, Greenberg EP, Welsh MJ. 2002. A component of innate immunity prevents bacterial biofilm development. *Nature.* 417:552-555.
- Song B, Leff LG. 2006. Influence of magnesium ions on biofilm formation by *Pseudomonas fluorescens*. *Microbiol Res.* 161: 355-361.
- Srinivas MRS, Chand N, Lonsane BK. 1994. Use of Plackett-Burman design for rapid screening of several nitrogen sources, growth/product promoters, minerals and enzyme inducers for the production of alpha-galactosidase by *Aspergillus niger* MRSS 234 in solid state fermentation system *Biopro Biosys Eng.* 10: 1615-7591
- Sutherland I. 2001. Biofilm exopolysaccharides: a strong and sticky framework. *Microbiology.* 147: 3-9.
- Tanji Y, Morono Y, Soejima A, Hori K, Unno H. 1999. Structural analysis of a biofilm which enhances carbon steel corrosion in nutritionally poor aquatic environments. *J Biosci Bioeng.* 88: 551-556
- Tiedje JM. 1994. Denitrifiers. In: Weaver RW, Angle JS, Bottomley PS (eds). *Methods of soil analysis. Part 2: Microbiological and biochemical properties.* Madison, Wisconsin: Soil Science Society of America. 245-267.
- Turakhia MH, Cooksey KE, Characklis WG. 1983. Influence of a calcium-specific chelant on biofilm removal. *Appl Env Microbiol.* 46: 1236-1238.

- Urakami Teizi, Hisaya Araki, Hiromi Oyanagi, Ken-Ichiro Suzuki, and Kazuo Komagata. 1990. *Paracoccus aminophilus* sp. nov. and *Paracoccus aminovorans* sp. nov. which utilize N, N-dimethylformamide. *Int J Sys Bac.* 40: 287-291
- Vasilyeva G K., Ludmila P, Bakhaeva, Elena R. Strijakova, Patrick J. S. 2003. Bioremediation of 3,4-dichloroaniline and 2,4,6-trinitrotoluene in soil in the presence of natural adsorbents. *Env Chem Lett.* 1:179–183
- Wimpenny JWT, Colasanti R. 1997. A unifying hypothesis for the structure of microbial biofilms based on cellular automaton models. *FEMS Microbiol Eco.* 22:1-16.
- Xu G, Zheng W, Li Y, Wang S, Zhang J, Yan Y. 2008. Biodegradation of chlorpyrifos and 3,5,6-trichloro-2-pyridinol by a newly isolated *Paracoccus* sp. strain TRP. *Int Biodet Biodeg.* 62: 51–56
- Yang L, Barken KB, Skindersoe ME, Christensen AB, Givskov M, Tolker-Nielsen T. 2007. Effects of iron on DNA release and biofilm development by *Pseudomonas aeruginosa*. *Microbiology.x* 153:1318-1328.